American Mineralogist, Volume 72, pages 1056–1070, 1987

Effects of B and H_2O on liquidus phase relations in the haplogranite system at 1 kbar

MICHEL PICHAVANT
Centre de Recherches Pétrographiques et Géochimiques, BP 20, 54501 Vandœuvre les Nancy, France

ABSTRACT

Liquidus phase relations have been determined in the system Qz-Ab-Or at 1 kbar with 1 and 4.5 wt% B_2O_3 in the melt under both H_2O-saturated conditions and H_2O-undersaturated conditions (4.5 wt% B_2O_3 in the melt), using a H_2O-CO_2 fluid mixture. Under H_2O-saturated conditions, the addition of B_2O_3 leads to a reduction of the liquidus temperatures for compositions in the feldspar field; compositions in the quartz field are not significantly affected. The minimum liquidus temperature is progressively reduced, and its composition moves toward the Ab corner: $Qz_{38}Ab_{33}Or_{29}$, 720 °C (B-free, Tuttle and Bowen, 1958), $Qz_{36}Ab_{37}Or_{27}$, 680 °C (1 wt% B_2O_3), $Qz_{31}Ab_{46}Or_{23}$, 640 °C (4.5 wt% B_2O_3). H_2O solubility in the melt increases with increasing B concentration. Isobaric reduction of the H_2O content in the melt by about 50% at constant B_2O_3 increases liquidus temperatures for all of the compositions studied and shifts the minimum liquidus composition toward the Qz-Or side at constant Qz contents: $Qz_{31}Ab_{34}Or_{35}$, 750 °C (4.5 wt% B_2O_3).

The contraction of the liquidus field for Ab suggests that the addition of B partially disrupts the aluminosilicate network. B-bearing structural units are formed involving alkalis (mainly Na) that were previously used for charge-balancing ^{IV}Al. A fraction of the B atoms may exist in tetrahedral coordination. The increase in the H_2O solubility is attributed to the hydrolysis of the borate units. An isobaric increase of the H_2O content of the melt has similar effects on phase relations, indicating that H_2O is preferentially associated with the Ab-forming components in the melt and that the incorporation of H_2O in aluminosilicate melts may involve expulsion of Al from the network. These results allow an estimation to be made of the individual effects of pressure and of the H_2O content of the melt on the phase relations in the Qz-Ab-Or system. The B concentration of natural magmas (1 wt% B_2O_3 maximum) is too low to influence significantly the major-element composition of residual melts. However, the minor- and trace-element chemistry of these melts may be profoundly affected.

INTRODUCTION

B is concentrated during the late stages of differentiation of felsic magmas, as shown by the presence of magmatic tourmaline in some leucogranites (Benard et al., 1985) and by the composition of fluid inclusions in some pegmatites (London, 1986). It has been demonstrated recently that the addition of B_2O_3 has marked effects on solidus temperatures (Chorlton and Martin, 1978; Pichavant, 1981) and on partitioning of elements between melt and vapor in the haplogranite system Qz-Or-Ab (Pichavant, 1981). Solidus temperatures are drastically reduced with the addition of B_2O_3 to H_2O, by more than 100 °C for some concentrations (Pichavant, 1981). B is partitioned toward the vapor phase relative to melt ($K_d = [B_2O_3]_{melt}/[B_2O_3]_{vapor} = 0.33$, Pichavant, 1981). With B present, aqueous vapor phases coexisting with melts become enriched in Na relatively to K, and the silicate solute content of the vapor phase is higher than with H_2O alone (Pichavant, 1981). These data are particularly relevant to vapor-present late magmatic and pegmatitic processes. However, they do not give much information about the effect of B on aluminosilicate melt structure, crystal ⇌ liquid equilibria, and the composition of residual melts in B-rich natural magmatic systems. Such information is presented in this paper along with experimental data on the effect of B on liquidus phase relations in the haplogranite system Qz-Or-Ab at 1 kbar.

Most of the new experimental data concern H_2O-saturated liquidus phase relations. However, H_2O-undersaturated phase relations were also studied, as it was found earlier (Pichavant, 1981) that the isobaric solubility of H_2O increases from B-free to B-bearing melts. Thus it is necessary to distinguish between the individual effects of B and H_2O on phase relations. This was achieved by determining part of the H_2O-undersaturated liquidus phase relations. Therefore, this study provides experimental information about the isobaric effect of H_2O on phase relations in the haplogranite system. It should be noted that the classical studies of Tuttle and Bowen (1958) and Luth et al. (1964) do not allow the effect of H_2O on phase

0003–004X/87/1112–1056$02.00

relations to be separated from that of pressure because the H_2O content of the melt and the pressure were simultaneously changed in their experiments. Given the now-general agreement that most granite magmas are H_2O-undersaturated and the current debate about H_2O solution mechanisms in aluminosilicate melts, it is obviously of great importance to have experimental information about the individual effect of H_2O on phase relations in the haplogranite system.

Experimental methods

Starting materials

Starting silicate materials were synthetic B-bearing glasses with various compositions in the Qz-Or-Ab system. These were made from gels prepared using conventional techniques from TEOS (Si), aluminum nitrate, and potassium and sodium carbonates. B was introduced as H_3BO_3. After drying, the gels were melted at 1400 °C in welded Pt capsules for 3 to 8 h (two cycles of melting with grinding in between). The starting glasses, analyzed for Si, Al, K, and Na by electron microprobe and for B by a wet-chemical method (discussed below; Table 1), do not deviate substantially from the Qz-Or-Ab plane. There is no significant compositional difference between various batches of glasses prepared from the same starting gel (Table 1). In this paper, liquidus phase relations have been studied for two average B_2O_3 concentrations in the melt, i.e., 1 and 4.5 wt% (see below). Because of the problem of the loss of B in the vapor phase (see below), each of the two series of starting glasses has been prepared with a slight excess of B_2O_3 compared to the desired concentration in the melt (glasses nos. 1–11: avg. 1.1 wt%; nos. 12–27: avg. 4.8 wt% B_2O_3; Table 1).

For the H_2O-saturated experiments [the initial mole fraction of H_2O in the fluid phase is 1, i.e., $X^{fl}_{H_2O}$ (in.) = 1], all charges consisted of 90% of silicate materials (~40 mg of glass ground to about 50 μm) plus 10% added water (doubly distilled, deionized H_2O). H_2O-undersaturated experiments were carried out with a H_2O-CO_2 fluid mixture. H_2O and $Ag_2C_2O_4$ were added in a proportion corresponding to 10% (H_2O + CO_2) for 90% of silicates (about 40 mg of ground glass). For these experiments, the initial fluid composition was fixed to $H_2O/(H_2O + CO_2)$ = 0.6 ± 0.02 mole fraction [$X^{fl}_{H_2O}$ (in.) = 0.6]. The charges were generally loaded in Au capsules (25 × 2.5 mm; thickness 0.2 mm) that were then welded. Pt capsules were also employed.

Apparatus and run procedure

Almost all runs were made in René-41 rapid-quench cold-seal pressure vessels. The longitudinal temperature gradients usually characteristic of these vessels were reduced by using special furnaces with windings condensed toward the colder end of the bomb and by working with Ar as the pressure medium. For each vessel-furnace pair, the hot-spot zone was determined under pressure by using a sheathed dual chromel-alumel thermocouple (calibrated against melting of NaCl and against a thermocouple calibrated and certified by the Laboratoire National d'Essais, Paris, France). With the vessel in the optimum position inside the furnace, maximum temperature gradients do not exceed 3 °C along 35 mm at 800 °C. Under run conditions, temperatures were measured by external unsheathed chromel-alumel thermocouples (also calibrated against melting of NaCl and against the certified thermocouple) and recorded permanently. The readings were corrected against the internal thermocouple (maximum correction usually less than ±5 °C with bombs in optimum position). Runs lasted up to 2 months with continuous monitoring (daily T fluctuation less than ±2 °C). The overall maximum error on the recorded temperatures is less than ±10 °C. Pressure was measured with a Heise Bourdon tube gauge (error ±0.020 kbar). Runs at 860 °C were carried out in an internally heated pressure vessel by Dr. D.A.C. Manning (University of Manchester).

Several capsules tied together were often loaded in the same bomb to allow direct comparison of results for different compositions. Heating time was usually between 30 and 60 min, with simultaneous rise of temperature and pressure from an initially applied pressure of 0.8–0.9 kbar. Capsules were quenched under pressure by tilting the bomb out of the furnace (quench time ≈ 5 s). After a check for leaks by weighing, the capsules were opened. The run products were examined by petrographic techniques using immersion oils and gypsum plate. Selected experimental glasses and liquidus feldspars were analyzed by electron microprobe for the construction of the conjugation lines and three-phase triangles. Care was taken to analyze charges having a minimum amount of crystals so that the liquid composition remained essentially in its constant B_2O_3 plane.

For each starting composition, forward runs were first conducted at decreasing temperature intervals of 20 °C up to the appearance of crystalline phases in the run products, as determined by petrographic observation. Reversal experiments consisted of two-stage runs. The initial temperature was one known from the forward runs to produce partial crystallization. Then, the temperature was raised isobarically to the final temperature and kept steady. Temperature intervals between two reversals are usually 10 °C. For a given composition, the *liquidus temperature* is located between the temperature of a run showing evidence of crystal growth (either a forward or a reversal experiment) and that of a reversal run yielding only glass or showing evidence of crystal dissolution.

Analytical techniques

Glasses (starting materials and glasses produced in the experiments) and feldspars were analyzed using the Camebax electron microprobe of the University of Nancy. Analytical conditions were acceleration voltage, 15 kV; sample current, 6 nA; counting time on peak, 6 s. The standards involved were albite, K-feldspar, and Al_2O_3, and ZAF correction procedures were used. To minimize the loss of K and Na during glass analysis, the beam was defocused to a size of 15 μm (2 μm for feldspar analyses). The resulting K_2O and Na_2O were all slightly corrected upward by using calibration curves constructed from glasses analyzed by wet-chemical techniques. The data in Tables 1, 5, and 6 are all averages of multiple analyses (starting glasses: about five spots each; experimental glasses: between two and five spots each; feldspars: between one and four crystals analyzed per sample).

The B content of the glasses was analyzed by colorimetry with carminic acid (Pichavant, 1981) with a maximum uncertainty of ±10%. In this paper, the B_2O_3 concentrations in glasses are given on an anhydrous basis only.

Results

Run products

Phases present in the run products include glass in all runs, quartz (doubly terminated hexagonal pyramids, size less than 5 μm), and alkali feldspars. No other crystalline phase was encountered in the present study. The feldspars grow mostly as euhedral tablets (average size, 5–15 μm).

TABLE 1. Composition of the starting glasses

	1	2	3	4	5	6	7	8	9	10	11	12	12*	13	14
SiO_2**	79.71	78.99	78.08	78.09	75.57	76.38	75.14	75.12	74.11	77.01	77.44	79.68	79.11	76.75	77.3
Al_2O_3	11.73	11.4	11.32	11.14	13.46	13.35	13.13	12.83	12.79	12.18	11.94	9.13	9.05	11.03	10.59
K_2O	1.64	3.36	5.05	6.6	1.74	3.03	4.96	6.46	8.17	4.39	4.76	3.1	3.14	1.55	3.1
Na_2O	5.68	4.61	3.42	2.52	6.97	5.89	4.62	3.51	2.41	4.0	3.76	3.44	3.28	5.65	4.48
B_2O_3†	1.13	1.17	1.19	1.17	1.14	1.1	1.07	1.0	0.95	1.19	1.19	4.85	5.02	4.78	4.45
Total	99.89	99.53	99.06	99.52	98.88	99.75	98.92	98.92	98.43	98.77	99.09	100.2	99.6	99.76	99.92
Qz	40.9	40.0	39.7	39.3	29.0	30.9	29.9	30.6	29.6	37.1	38.2	50.1	50.8	39.9	41.7
Or	9.8	20.2	30.5	39.1	10.5	18.2	30.0	39.0	49.5	24.2	28.7	19.2	19.6	9.6	18.9
Ab	48.7	39.7	29.6	21.4	60.3	50.5	40.0	30.3	20.9	38.1	32.5	30.5	29.3	50.4	39.2
Co	0.6	0.1	0.2	0.0	0.1	0.4	0.1	0.1	0.0	0.6	0.6	0.1	0.3	0.1	0.0
KS	0.0	0.0	0.0	0.1	0.0	0.0	0.0	0.0	0.0	0.0	0.0	0.0	0.0	0.0	0.1
NaS	0.0	0.0	0.0	0.1	0.0	0.0	0.0	0.0	0.0	0.0	0.0	0.0	0.0	0.0	0.1

Note: Qz = quartz, Or = orthoclase, Ab = albite, Co = corundum, KS = K_2SiO_3, NaS = Na_2SiO_3, n.d. = not determined.
* Same glass, different batches.
** Average of five microprobe analyses for each glass, uncertainties 0.7% (SiO_2), 1.8% (Al_2O_3), 3% (K_2O), 4.5% (Na_2O).
† Analyzed by wet-chemical techniques (see text).

Skeletal feldspars were also encountered irrespective of temperature and B_2O_3 concentration. The silicate melt always quenched to a fluid inclusion–rich colorless glass. No evidence of liquid immiscibility was found, in agreement with the results of Pichavant (1981). A vapor phase is present in all runs as indicated by release of a small amount of aqueous solution on opening [runs with 1 wt% B_2O_3, $X^{Fl}_{H_2O}$ (in.) = 1], by swollen capsules, hissing when punctured [runs with 4.5 wt% B_2O_3, $X^{Fl}_{H_2O}$ (in.) = 0.6] or by the presence of numerous fluid inclusions trapped in glass for all charges. Runs with 4.5 wt% B_2O_3 and $X^{Fl}_{H_2O}$ (in.) = 1 appeared "dry" on opening.

In the present study, no attempt was made to analyze the vapor phase (see Pichavant, 1981). The starting Qz-Or-Ab composition is not modified by incongruent dissolution (as indicated by the microprobe analysis of some glasses above the liquidus) because the vapor phase is present only in very small amounts. In spite of that, B is lost in significant quantities to the vapor phase. Borate daughter crystals appear in fluid inclusions for all experiments with 4.5 wt% B_2O_3 in the melt and $X^{Fl}_{H_2O}$ (in.) = 1 (see also Pichavant, 1981). Mass-balance calculations of the distribution of B between melt and vapor phases (using the average B_2O_3 content of each of the two series of starting glasses, $K_d = 0.33$, and the proportion of phases present in the charge) yield 2.9 and 12.8 wt% B_2O_3 (vapor), 1 and 4.5 wt% B_2O_3 (melt) for experiments with $X^{Fl}_{H_2O}$ (in.) = 1. These vapor-phase concentrations (0.7 and 3.7 mol% B_2O_3) suggest that in experiments with $X^{Fl}_{H_2O}$ (in.) = 1, the fugacity of H_2O does not significantly differ from the fugacity of pure H_2O under the same T and P (i.e., $a_{H_2O} \simeq 1$). In contrast, for experiments with $X^{Fl}_{H_2O}$ (in.) = 0.6, the fugacity of H_2O in the vapor phase is strongly reduced (i.e., $a_{H_2O} < 1$).

Analysis of the B content of an experimental glass above the liquidus (no. 25, T = 740 °C, Table 3) yielded B_2O_3 = 4.57 wt%, in agreement with the concentration in the melt calculated from mass balance (4.5 wt%). Thus, the experimental method adopted (small amount of vapor phase present in the charge and starting glasses with B contents exceeding the desired values) was able to successfully control the B concentration in the experimental melts. The presence of CO_2 increases K_d (the absence of borates in fluid inclusions tells that B partitions more in favor of the melt), and B concentrations in H_2O-CO_2 experiments should be slightly higher, although identical within error to those in H_2O-saturated experiments.

H_2O-saturated liquidus phase relations

Experimental results for $X^{Fl}_{H_2O}$ (in.) = 1 and 1 and 4.5 wt% B_2O_3 in the melt are given in Tables 2 and 3. Analytical data for feldspars and coexisting glasses are given in Tables 5 and 6. Liquidus phase relations are represented in Figures 1 and 2. In spite of slight nonternary behavior (the melts have dissolved H_2O and B_2O_3; also the vapor phase contains B and some dissolved silicates), a ternary isobaric representation of the phase relations has been adopted for each of the two B_2O_3 concentrations investigated. Thus the diagrams represent two isobaric sections in 5-dimensional space for two B_2O_3 contents in the melt (1 and 4.5 wt%) and for their corresponding H_2O contents at saturation ($a_{H_2O} \simeq 1$).

Liquidus temperature brackets are never larger than 20 °C except for composition no. 7 (Table 2). In the latter, the liquidus temperature is probably close to 740 °C, as it was not clear whether the crystals were growing or dissolving in the 710 → 740 °C reversal experiment [compare with compositions no. 4 (liquidus temperature 750 °C), no. 5 (790 °C) in Table 2 or no. 16 (730 °C) in Table 3]. For most compositions, in particular all those with 4.5 wt% B_2O_3, the maximum temperature difference between the appearance of crystals in the forward experiments and their disappearance in the reversals is 20 °C. Compositions with 1 wt% B_2O_3 in the feldspar field exhibit larger discrepancies (up to a maximum of 40 °C between forward and reversal runs, Table 2). This indicates a small problem of supercooling in the forward runs. Because of that problem, the liquidus temperatures for the 1 wt% B_2O_3 compositions have been bracketed by reversals only (Table 2). The conjugation lines and three-phase triangles also point to some problems of super-

TABLE 1.—*Continued*

15	16	17	18	18*	18*	19	19*	20	21	22	23	24	25	26	27
75.99	74.56	73.66	73.32	73.96	73.37	72.51	73.49	72.58	71.7	71.2	70.75	69.38	70.5	69.32	69.01
10.68	10.74	12.82	12.65	12.89	12.83	12.51	12.71	12.48	12.33	14.7	14.42	14.55	14.09	14.34	14.09
4.55	6.15	1.54	3.17	3.16	3.24	4.53	4.75	6.15	7.45	1.6	3.08	4.75	6.08	8.25	9.2
3.49	2.27	6.85	5.7	5.87	5.84	4.63	4.49	3.31	2.32	7.85	7.03	5.79	4.45	3.33	2.43
4.55	4.98	4.67	4.7	n.d.	n.d.	4.89	n.d.	4.74	5.39	4.84	5.05	4.44	4.74	4.74	4.92
99.26	98.7	99.54	99.54	95.89	95.28	99.07	95.44	99.26	99.19	100.19	100.33	98.91	99.86	100.01	99.65
40.4	40.4	29.8	30.1	29.5	29.2	30.0	30.6	31.5	31.7	20.4	20.5	18.9	22.4	19.5	20.8
28.4	38.8	9.5	19.5	19.2	19.7	28.4	29.4	38.5	46.9	9.9	18.5	29.5	37.8	50.9	57.4
31.2	20.4	60.6	50.2	51.1	50.7	41.6	39.8	29.6	20.9	69.7	60.4	51.5	39.6	29.5	21.7
0.0	0.4	0.0	0.0	0.0	0.0	0.0	0.2	0.4	0.5	0.0	0.0	0.0	0.2	0.0	0.1
0.0	0.0	0.0	0.1	0.1	0.1	0.0	0.0	0.0	0.0	0.0	0.2	0.0	0.0	0.1	0.0
0.0	0.0	0.1	0.1	0.2	0.3	0.0	0.0	0.0	0.0	0.0	0.4	0.1	0.0	0.0	0.0

cooling and incomplete nucleation and growth in the forward experiments: (1) the temperatures indicated by the ends of the conjugation lines and three-phase triangles (mainly determined in forward experiments) are generally lower than the actual run temperatures (Figs. 1 and 2); (2) the experimental melts in most cases plot close to the starting compositions, indicating a proportion of crystals generally smaller than the equilibrium proportion (Figs. 1 and 2). This is true also for the H_2O-undersaturated experiments (Fig. 4). Exceptions are two crystal-rich charges (nos. 17 and 22, Fig. 2 and Table 6) that plot far away from their starting compositions and are possibly outside the 4.5 wt% B_2O_3 plane.

Mass balance between reactants and products is satisfied if account is taken of the analytical errors on the glass compositions: feldspars, glasses, and starting compositions are roughly colinear; three-phase triangles generally enclose the starting compositions (see also the H_2O-undersaturated experiments, Fig. 4). The compositions of the experimental glasses do not depart from the Qz-Or-Ab plane in any types of experiments (Table 6).

Structural formulae of the liquidus alkali feldspars (Table 5) do not reveal any reproducible anomaly that can be attributed to the substitution of B for Al in the feldspars (Pichavant et al., 1984, and references therein). Si is usually in slight excess, possibly because of some glass contamination. However, alkali/Al ratios are close to one. Thus, there appears no detectable Al deficiency in these feldspars. However, this does not preclude that B could be present at the 100–1000 ppm level.

The addition of B leads to a reduction of liquidus temperatures for some compositions. In particular, all compositions in the feldspar field have reduced liquidus temperatures for both B_2O_3 contents. Comparing with B-free compositions at 1 kbar (Tuttle and Bowen, 1958), reductions are on the order of 30–50 °C for 1 wt% B_2O_3 and 120–150 °C for 4.5 wt% B_2O_3. In contrast, compositions in the quartz field do not have reduced liquidus temperatures (Fig. 3). The quartz liquidus is not significantly different for B-free and for B-bearing compositions. This contrasts with the increase of quartz liquidus temperatures with F content, as observed in the same system (Manning, 1981, and Fig. 3).

Temperatures and compositions of the minimum liquidus-temperature points for 1 and 4.5 wt% B_2O_3 and $X^{Fl}_{H_2O}$ (in.) = 1 are given in Table 7. For both B_2O_3 sections, the quartz-feldspar field boundaries are located from the experiments, and the position of the thermal minima along these field boundaries (minimum liquidus compositions) is bracketed from three-phase triangles. Temperatures of these minimum liquidus compositions are given by the intersection of the quartz and feldspar liquidi (Fig. 3). Compared to the B-free system at the same pressure (Tuttle and Bowen, 1958), the reductions of the minimum temperatures are 40 and 80 °C for 1 and 4.5 wt% B_2O_3, respectively. The minimum liquidus temperature for 4.5 wt% B_2O_3 (640 °C, Table 7) lies below the critical temperature of the disordered alkali feldspar solvus (about 660 °C, Smith and Parsons, 1974; Lagache and Weisbrod, 1977). Therefore, a change from minimum-type to eutectic-type phase relations must occur between the 1 and 4.5 wt% B_2O_3 sections. Although not experimentally determined, the two feldspar–liquid-vapor equilibrium has been represented in Figure 2 as a line originating from the minimum liquidus point up to the 660 °C isotherm on the liquidus surface. Figures 1 and 2 clearly show that the minimum liquidus-temperature points are progressively shifted toward the Ab corner with increasing B_2O_3.

The H_2O contents of the experimental glasses have not been systematically determined. However, Pichavant (1981) has demonstrated an increase of the solubility of H_2O with increasing B_2O_3 contents for compositionally identical melts. In this study, the absence of detectable free aqueous solution at the opening of the charges with 4.5 wt% B_2O_3 and $X^{Fl}_{H_2O}$ (in.) = 1 is further indication of higher H_2O solubilities in melts with 4.5 wt% B_2O_3. Estimations of the H_2O contents of melts with 1 and 4.5 wt% B_2O_3 from the data of Pichavant (1981) yield, respectively, 4.5–5 and 6–6.5 wt% H_2O (Table 7). A determination of the H_2O content of composition no. 18 (800 °C), carried out by the weight-loss method, yielded 6.16 wt% H_2O.

TABLE 2. Experimental results for 1 wt% B_2O_3, $X^{Fl}_{H_2O}$ (in.) = 1.0

Glass no.	Temp (°C)	Duration (h)	Results	Feldspar comp. (mol% $KAlSi_3O_8$)
1	780	240	L	
	760	192	L + Qz	
	760→770	168→192	L + Qz (grow.)	
	760→780	168→168	L + Qz (diss.)	
	760→790	240→288	L	
2	770	240	L	
	760	192	L + (Qz)	
	740	192	L + Qz	
	750→770	168→168	L + Qz (grow.)	
	750→780	240→288	L	
3	760	240	L	
	740	192	L + Qz	
	740→750	168→192	L + Qz (grow.)	
	740→760	168→168	L + Qz (diss.)	
	740→770	240→288	L	
4	760	192	L	
	740	192	L + (Qz)	
	720	312	L + Qz	
	740→750	168→192	L + (Qz) (grow.?)	
	740→760	168→168	L	
	730→760	168→168	L	
5	800	68	L	
	780	192	L + (Sa)	
	780→790	96→144	L + (Sa) (grow.?)	
	780→800	168→168	L	
6	760	192	L	
	740	192	L + (Sa)	
	720	312	L + Sa	8
	740→750	168→192	L + (Sa) (grow.?)	
	740→760	168→168	L	
7	740	192	L	
	720	312	L + (Sa)	
	700	312	L + Sa	56
	700→710	168→192	L + Sa (grow.)	55
	710→740	240→288	L + (Sa) (grow.?)	
8	760	240	L	
	740	192	L + Sa	78
	740→750	168→192	L + Sa (grow.)	80
	740→760	168→168	L + Sa (grow.)	
	750→770	240→288	L + Sa (grow.?)	
	750→780	168→192	L	
9	800	68	L + (Sa)	
	780	192	L + Sa	89
	800→810	96→144	L + (Sa) (grow.?)	
	800→820	96→72	L	
10	720	168	L	
	700	312	L + (Qz)	
	680	288	L + Qz + Sa	22
	680→700	336→288	L + Qz + Sa (grow.?)	
	680→720	336→336	L + (Qz) (diss.)	
11	720	168	L	
	700	312	L + (Qz)	
	680	288	L + Qz + Sa	67
	680→700	336→288	L + Qz + Sa (grow.?)	
	680→720	336→336	L + (Qz) (diss.)	

Note: Qz = quartz, Sa = alkali feldspar solid solution, L = liquid, ( ) = trace amount, (diss.) = crystals dissolving, (grow.) = crystals growing. Vapor phase present in all runs.

H_2O-undersaturated liquidus phase relations

Experimental results for $X^{Fl}_{H_2O}$ (in.) = 0.6 and 4.5 wt% B_2O_3 in the melt are given in Table 4. The analytical data for feldspars and coexisting glasses are in Tables 5 and 6. Liquidus phase relations are represented in Figure 4. The phase diagram of Figure 4 is a ternary isobaric section for 4.5 wt% B_2O_3 in the melt and a given H_2O content in the melt. The latter is fixed by the composition of the H_2O-CO_2 vapor phase but also by the proportion of $H_2O + CO_2$ and silicates in the charge (Wyllie and Tuttle, 1960, 1961; Boettcher, 1984). In this study, care was taken to keep constant the proportion of $H_2O + CO_2$ in the starting materials. The H_2O content of the melt was determined by mass balance from the amount of H_2O and CO_2 in the vapor and melt phases before and after the experiment. The vapor-phase composition was obtained from the microthermometric study of the three-phase fluid inclusions (liquid H_2O, liquid and vapor CO_2, Pichavant and Ramboz, 1985a, 1985b). The vapor-phase composition changes from $H_2O = 60 \pm 2$, $CO_2 = 40 \pm 2$ (starting composition) to $H_2O = 35 \pm 5$, $CO_2 = 62 \pm 5$, $CH_4 = 3 \pm 1$ (mol%, determined in glass no. 19, $T = 780$ °C, Table 4). The presence of CH_4 indicates partial reduction of the starting H_2O-CO_2 mixture (the f_{O_2} imposed by the pressure vessel ranges between Ni-NiO and MnO-Mn_3O_4; Montel, 1986). The obtained H_2O content of the melt (assuming CO_2 to be insoluble in the melt) is 2.8 ± 0.4 wt%, in reasonable agreement with H_2O contents calculated from the Burnham (1979) model (2.0–2.4 wt% H_2O, written comm., C. Wayne Burnham and H. Nekvasil).

Liquidus temperatures have been determined for four starting compositions selected because they are close to the field boundary determined under H_2O-saturated conditions (Fig. 2). Temperature brackets are 20 °C except for composition no. 21. The latter has not been properly bracketed (Table 4), and the liquidus temperature was assumed to be close to 840 °C. Except for that composition, the maximum difference in temperature between the appearance of crystals (forward experiments) and their disappearance (reversals) is 20 °C. Determination of the liquidus temperatures is slightly more difficult because the H_2O-undersaturated subliquidus charges carry a smaller percentage of crystals than in the H_2O-saturated experiments.

Reduction of the H_2O content of the melt at constant B_2O_3 increases liquidus temperatures for the four compositions studied. The maximum rise in temperature is for compositions nos. 18 and 19 (about 120 °C). Figure 3 shows that compositions in the quartz field are affected as much as compositions in the feldspar field. Composition no. 19 has quartz as a liquidus phase, whereas feldspar is the liquidus phase under H_2O-saturated conditions. However, there is no significant displacement of the quartz-feldspar field boundary compared to H_2O-saturated conditions. The thermal minimum along the field boundary is bracketed by three-phase triangles. Its composition (Table 7) is shifted away from the H_2O-saturated minimum toward the Qz-Or sideline. The observed shift

TABLE 3. Experimental results for 4.5 wt% B_2O_3, $X^{fl}_{H_2O}$ (in.) = 1.0

Glass no.	Temp (°C)	Duration (h)	Results	Feldspar comp. (mol% $KAlSi_3O_8$)
12	860*	168	L	
	840	18	L + Qz	
	820→860*	72→168	L	
13	780	144	L	
	760	288	L + Qz	
	750→770	168→168	L + Qz (diss.)	
	750→780	336→312	L	
14	780	144	L	
	760	216	L + (Qz)	
	740	264	L + Qz	
	740→760	240→288	L + Qz	
	740→770	168→168	L + Qz (grow.)	
	740→780	336→312	L	
15	760	288	L	
	740	288	L + Qz	
	740→750	192→312	L + Qz (diss.?)	
	740→760	168→384	L + (Qz)	
16	740	168	L	
	720	312	L + Qz	
	720→730	288→312	L + Qz (grow.?)	
	720→740	288→312	L	
17	720	240	L	
	700	312	L + Qz + Sa	3
	700→720	240→240	L + (Sa) (diss.)	
	700→730	240→240	L	
18	680	528	L	
	660	528	L + (Sa)	
	650	624	L + Qz + Sa	6
	650→660	336→456	L + Qz + Sa	
	650→670	336→456	L + (Qz) + Sa	
	650→680	336→456	L + (Qz) + Sa (diss.)	
19	680	480	L	
	660	480	L + (Sa)	
	650	744	L + Qz + Sa	66
	650→670	744→696	L + (Qz?) + Sa (diss.)	
20	700	456	L	
	680	456	L + Sa	81
	680→690	480→936	L + Sa (grow.?)	
	680→700	672→504	L	
21	740	168	L	
	720	312	L + Sa	90
	720→740	216→312	L + Sa (diss.)	
22	760	288	L	
	740	288	L + Sa	2
	740→750	192→312	L + Sa (diss.?)	
	740→760	168→384	L + Sa (diss.)	
23	740	288	L	
	720	456	L + Sa	6
	720→740	240→264	L + (Sa) (diss.)	
24	720	240	L	
	700	312	L + Sa	17
	700→710	288→312	L + Sa (diss.)	
	700→720	480→2(	L + (Sa) (diss.)	
25	740	360	L	
	720	360	L + Sa	74
	720→740	240→288	L + (Sa) (diss.)	
	720→750	240→240	L	
26	780	360	L + (Sa?)	
	760	360	L + Sa	
	760→780	240→288	L + Sa (diss.)	
	760→790	336→312	L + (Sa) (diss.)	
27	800	120	L	
	780	96	L + Sa	91
	780→790	144→144	L + Sa (grow.?)	
	780→800	144→96	L + (Sa) (diss.)	

Note: Qz = quartz, Sa = alkali feldspar solid solution, L = liquid, ( ) = trace amount, (diss.) = crystals dissolving, (grow.) = crystals growing. Vapor phase present in all runs.

* Experiment in internally heated vessel.

is at approximately constant normative-quartz content. The temperature of the minimum liquidus composition, obtained from the intersection of the quartz and feldspar liquidus (Fig. 3), increases from 640 °C (H_2O-saturated) to 750 °C (H_2O-undersaturated, Table 7).

Discussion of the experimental data

Evaluation of equilibrium

The question of the attainment of equilibrium during experimental melting or crystallization of granitic compositions deserves detailed discussion (e.g., Johannes, 1980). In these liquidus experiments, two critical reaction mechanisms take place: (1) production of an homogeneous hydrous melt by diffusion of H_2O from the vapor phase into the initially "dry" starting glass and (2) nucleation and growth of crystalline phases in the hydrous melt. In order to discuss the attainment of equilibrium in these experiments, it is important to evaluate the kinetics of each of these two mechanisms.

With an average initial grain size of 50 μm for the starting ground glass, times of a few tens of minutes are sufficient for H_2O to diffuse throughout ($D_{H_2O} = 3.10^{-8}$ $cm^2 \cdot s^{-1}$, Shaw, 1974). Evidence of an homogeneous distribution of H_2O in the melt is furnished (1) by the homogeneous distribution of quartz and feldspar in subliquidus experiments and (2) by the fluid inclusions in glasses. The population of fluid inclusions is in all cases extremely homogeneous (with respect to phase assemblage and volumetric proportions), not only for a given experiment, but also for a given type of experiment. Thus, dissolution and homogenization of H_2O by diffusion in the melt takes place rapidly. This is also true for the H_2O-undersaturated experiments because of the use of a free fluid phase (H_2O-CO_2) to control H_2O fugacities. In comparison, the nucleation of silicate phases requires a much longer period of time. For alkali feldspars, nucleation lag times of several days have been commonly found in the systems Or-Ab-H_2O and Or-Ab-An-Qz-H_2O (Fenn, 1977; Swanson, 1977). For quartz, nucleation lag times ranging from several hours to a few days are reported by Swanson and Fenn (1986) in the system Ab-Qz-H_2O and for the Harding pegmatite composition. It is therefore concluded that crystallization did not start before H_2O homogenization was achieved by diffusion in the melt.

With the exception of the supercooling and nucleation problems noted previously, there is overall agreement be-

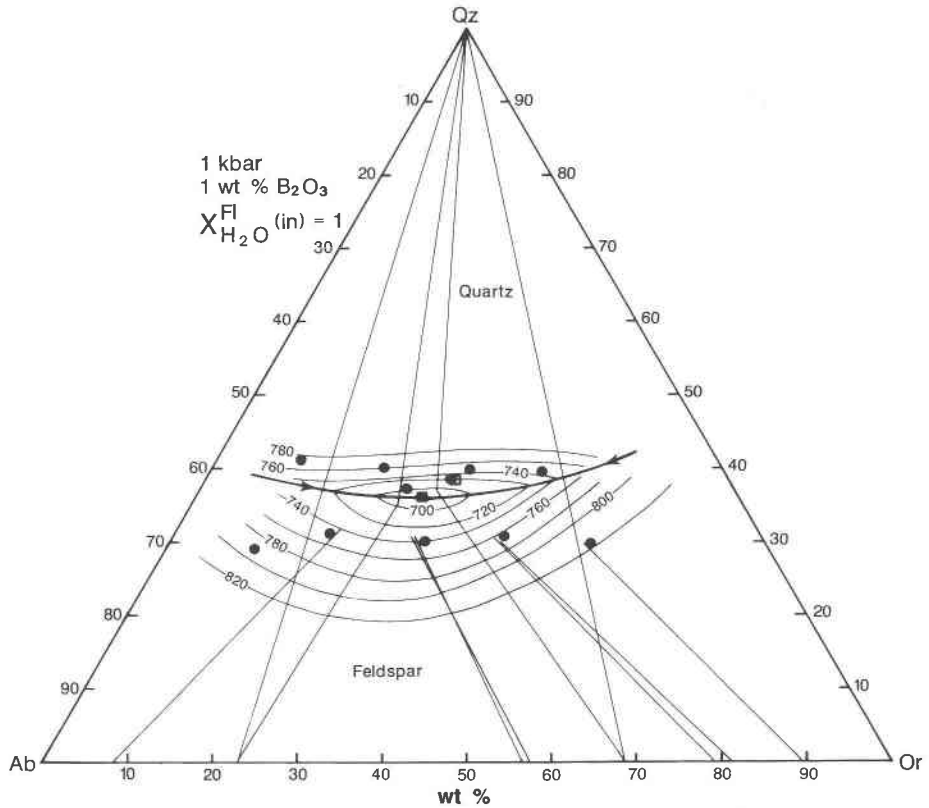

Fig. 1. Liquidus phase relations in the system Qz-Ab-Or at 1 kbar for 1 wt% B_2O_3 in the melt under H_2O-saturated conditions (see text). Isotherms labeled in °C. ● = compositions investigated (Table 1); ■ = minimum liquidus point of this system; □ = ternary minimum in the B-free system at 0.98 kbar (Tuttle and Bowen, 1958). Data for the construction of conjugation lines and three-phase triangles in Tables 5 and 6.

tween the forward and the reversal experiments. This is strong indication that equilibrium is approached. Supercooling is minor for most runs; complete nucleation and growth is not necessary for bracketing liquidus temperatures, as only the direction of reaction is required. On the other hand, superheating problems are not expected in the reversal runs, given the small and homogeneous size of the near-liquidus crystalline phases in the forward experiments. Owing to the rapid diffusion of Na and K in the alkali feldspars, run durations as in these experiments are long enough to approach equilibrium alkali distribution between melt and alkali feldspars (e.g., Johannes, 1985). An approach toward equilibrium is suggested by the chemical homogeneity of the run products. For a given sample, microprobe data for feldspars and experimental glasses are very constant (see above for the vapor phase). There is no great difference in the composition of feldspars and glasses, whether analyzed in forward or reversal runs (Table 2). However, complete chemical equilibrium is not attained, and partial equilibrium (exchange equilibrium, Thompson and Waldbaum, 1968) must prevail for compositions showing the largest supercooling. The euhedral shapes of quartz and feldspars indicates textural equilibrium between melt and crystals. Furthermore, the dominant crystal morphologies are consistent with small values of undercooling (Fenn, 1977; Swanson and Fenn, 1986).

In summary, the experiments closely approached equilibrium with respect to the determination of liquidus phases and temperatures, but complete crystal ⇌ liquid chemical equilibrium is not claimed.

Individual effects of B and H_2O on phase relations in the haplogranite system

The experimental data presented above describe the effect of two components, H_2O and B_2O_3, on phase relations in the haplogranite system Qz-Ab-Or. There is evidence of a complex interplay between these two components, as indicated for example by the increase of the H_2O solubility in the melt accompanying the increase in the B content. Before discussing the structural role of B and H_2O in aluminosilicate melts, it is necessary to identify the individual effects of each of these components on phase relations in the haplogranite system. In the following it is assumed that CO_2 does not dissolve significantly in the melt under the present experimental conditions; consequently no significant effect of CO_2 on melt structure is expected. This first-order approximation is supported by the composition of fluid inclusions in H_2O-CO_2 experiments and by mass-balance calculations (see above).

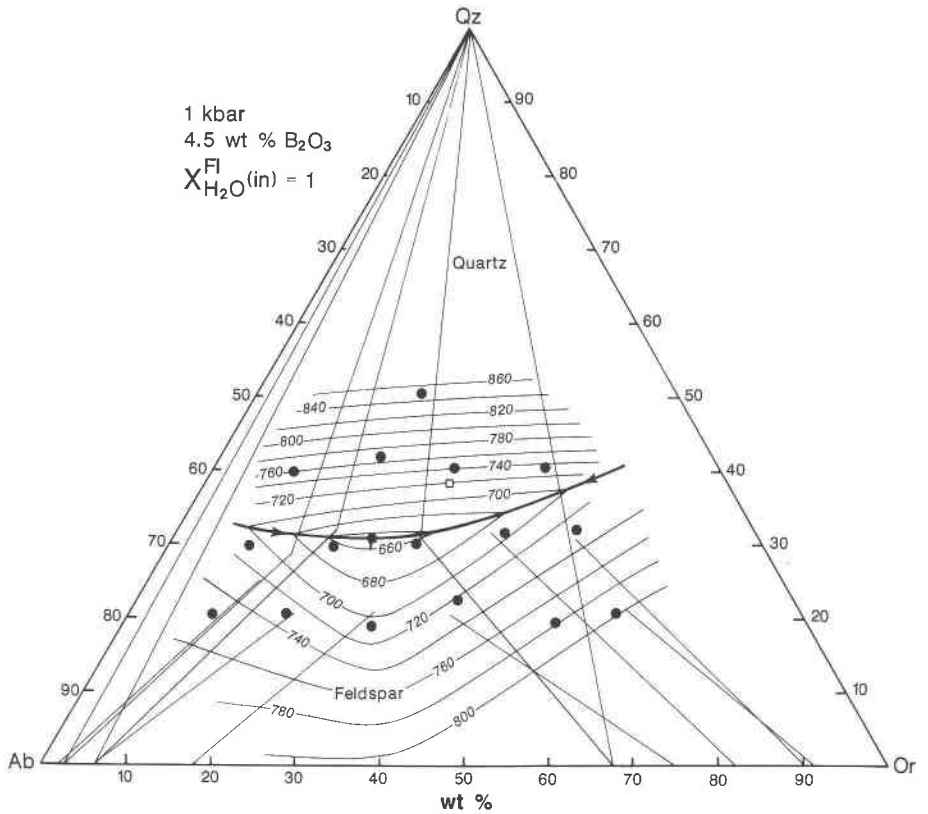

Fig. 2. Liquidus phase relations in the system Qz-Ab-Or at 1 kbar for 4.5 wt% B_2O_3 in the melt under H_2O-saturated conditions (see text). Notations, symbols, and sources of data as in Fig. 1. Note the two-feldspar field boundary drawn from the minimum liquidus point up to the 660 °C isotherm on the liquidus surface (see text).

Phase relations have been determined at 1 kbar in the system Qz-Ab-Or for 4.5 wt% B_2O_3 in the melt, both under H_2O-saturated (Fig. 2) and H_2O-undersaturated conditions (Fig. 4). The compositions of the corresponding minimum liquidus points are plotted in Figure 5. An isobaric increase of the H_2O content in the melt leads to a shift of the minimum liquidus composition toward the Qz-Ab side, at approximately constant Qz content. Though this shift is related to a significant decrease in the liquidus temperatures (see above), it is concluded that it mainly corresponds to the effect of isobarically increasing the H_2O content of the aluminosilicate network portion of the melt ("H_2O effect"). The shift observed in the B-bearing system is similar in direction to that estimated in the B-free system at 4 kbar (Steiner et al., 1975), also represented in Figure 5. A similar shift can be deduced from Whitney's (1975) 8-kbar phase diagram for his synthetic granite composition and from the 5-kbar field boundaries estimated by Huang and Wyllie (1975) in the Qz-Ab-Or-H_2O system. This "H_2O effect," as determined experimentally in the B-bearing system, conflicts with calculations that predict a shift of the minimum liquidus compositions toward the Qz apex (away from the feldspar join) with isobarically increasing H_2O content of the melt (Burnham and Nekvasil, 1986; Nekvasil and Burnham, 1987).

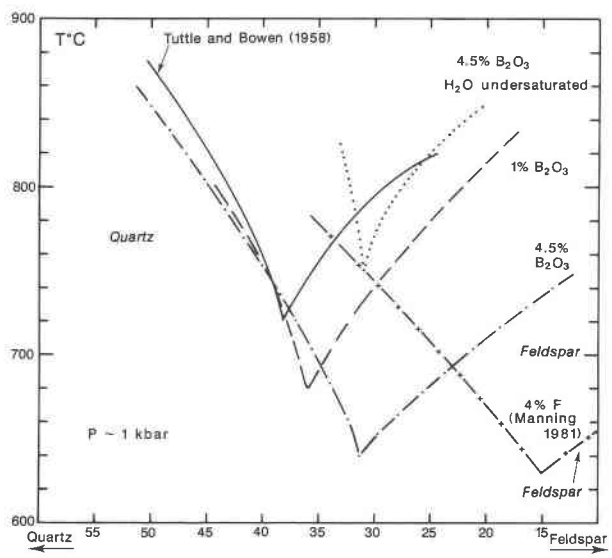

Fig. 3. Sections of the system Qz-Ab-Or-H_2O from the Qz apex through the minimum liquidus compositions to the feldspar join showing the effect of B and H_2O (this study), and of F (Manning, 1981) on the quartz and feldspar liquidi. H_2O-saturated conditions except when otherwise stated.

TABLE 4. Experimental results for 4.5 wt% B_2O_3, $X^{Fl}_{H_2O}$ (in.) = 0.6

Glass no.	Temp. (°C)	Duration (h)	Results	Feldspar comp. (mol% $KAlSi_3O_8$)
18	800	72	L	
	800	168	L	
	780	144	L + Qz + Sa	6
	780→800	144→72	L	
19	800	24	L	
	800	168	L	
	780	144	L + (Qz)	
	760	144	L + Qz + (Sa)	
	740	216	L + Qz + Qa	23
	780→800	144→72	L	
20	780	168	L	
	760	216	L + Sa	74
	740	384	L + Qz + Sa	71
	760→780	192→168	L	
21	800	144	L + (Sa)	
	780	216	L + Sa	
	760	216	L + Sa	87
	800→820	144→48	L + Sa (grow.)	

Note: Qz = quartz, Sa = alkali feldspar solid solution, L = liquid, ( ) = trace amount, (grow.) = crystals growing. Vapor phase present in all runs.

As noted previously, an increase in the B content is accompanied by an increase in the solubility of H_2O in the melt. Consequently, the change in phase relations with the addition of B_2O_3 under H_2O-saturated conditions should reflect the combined effects of B and H_2O: with progressively increasing B_2O_3, the H_2O-saturated minimum liquidus compositions are shifted toward the Ab corner, with a corresponding reduction of the minimum liquidus temperatures (Fig. 5). As the isobaric solubility of H_2O is known to be much higher in borate melts than in silicate melts (Franz and Scholze, 1963; Franz, 1966), the observed increase of the H_2O content of the melt is attributed to the hydrolysis of borate groups (see below). Considering that the borate and aluminosilicate groups form largely separate units in the melt (see below), the hydrolysis of the borate units will not greatly affect the aluminosilicate network portion in the melt. Therefore, it is the progressive addition of B to the system that is mainly responsible for the observed change in phase relations under H_2O-saturated conditions at 1 kbar ("B effect"). Comparison of the "H_2O effect" and "B effect" (Fig. 5) shows that they are different.

Structural role of B in aluminosilicate melts

This section is a discussion of the structural role of B in aluminosilicate melts from the phase relations determined above and from spectroscopic information (early studies reviewed by Pichavant, 1983a).

There is no evidence from this study for the incorporation of B into the aluminosilicate network. From the comparison of the Raman spectra of borosilicate and aluminosilicate glasses of feldspar composition, Konijnendijk (1975a) found a strong difference between Al, mainly incorporated in the network, and B, grouped in metaborate units not forming part of the network (see also Pichavant, 1983a). Electron microscopy of similar glasses (Konijnendijk, 1975b) suggests an irregular phase-separated structure, indicating agglomeration to some extent of the metaborate groups (see Pichavant, 1983a, for a description of the different borate units). These results are consistent with the recent NMR spectroscopic and oxide-melt solution calorimetric study performed along the join $NaAlSi_3O_8$-$NaBSi_3O_8$ (Oestrike et al., 1986) that indicates the presence of clustering into regions consisting of a tetrahedral network and regions dominated by borate units with ^{III}B. The compositions of the liquidus alkali feldspars analyzed in this study do not reveal the presence of large amounts of B in the feldspar structure, which suggests that B atoms are not significantly incorporated into the aluminosilicate network.

The coordination state of B in melts and quenched glasses obtained in this study is strongly related to the coordination of Al. Konijnendijk (1975b) has shown that the addition of Al_2O_3 to M_2O-B_2O_3-SiO_2 glasses (M = Na or K) lowers the proportion of ^{IV}B present. Because of the higher field strength of Al, the alkali ions previously used to charge-balance ^{IV}B become bonded to AlO_4 tetrahedra and a proportion of the B atoms is forced to the threefold coordination (see Pichavant, 1983a). In this study, the Qz-Ab-Or compositions are metaluminous [i.e., $Al_2O_3/(Na_2O + K_2O)$ is close to 1]. Thus, if most of the

TABLE 5. Composition of the alkali feldspars

Glass no.:	6	7	7	8	8	9	10	11	17	18	18	19	19	20	20
Temp (°C):	720	700	710	740	750	780	680	680	700	650	780	650	740	680	740
n:	2	2	2	2	2	1	1	1	3	2	1	1	1	1	2
SiO_2	68.72	66.43	66.35	65.07	64.79	65.12	67.37	67.24	68.46	67.61	67.83	66.12	68.78	66.41	65.52
Al_2O_3	19.01	18.56	18.81	18.32	18.27	18.12	18.24	18.35	18.97	19.21	18.63	18.98	19.19	17.58	18.25
K_2O	1.41	9.74	9.51	13.37	13.42	15.01	3.77	11.28	0.5	0.96	1.00	11.65	3.93	13.02	12.24
Na_2O	10.71	4.98	5.19	2.47	2.22	1.22	8.55	3.72	10.92	10.83	10.47	3.87	8.67	1.96	3.23
Total	99.85	99.71	99.86	99.23	98.7	99.48	97.97	100.58	98.85	98.61	97.93	100.62	100.57	98.98	99.24
Structural formulae calculated on the basis of 16 oxygens															
Si	6.03	6.02	6.0	6.0	6.01	6.02	6.07	6.05	6.04	6.0	6.05	5.98	6.03	6.1	6.02
Al	1.97	1.98	2.0	1.99	2.0	1.98	1.94	1.95	1.97	2.01	1.96	2.02	1.98	1.9	1.98
K	0.16	1.13	1.1	1.57	1.59	1.77	0.43	1.3	0.06	0.11	0.11	1.34	0.44	1.53	1.43
Na	1.82	0.87	0.91	0.44	0.40	0.22	1.49	0.65	1.87	1.86	1.81	0.68	1.48	0.35	0.58
$KAlSi_3O_8$ (mol%)	8	56	55	78	80	89	22	67	3	6	6	66	23	81	71

Note: *n* = number of microprobe analyses; uncertainties are 0.5% (SiO_2), 1.2% (Al_2O_3), 5% (Na_2O and K_2O).

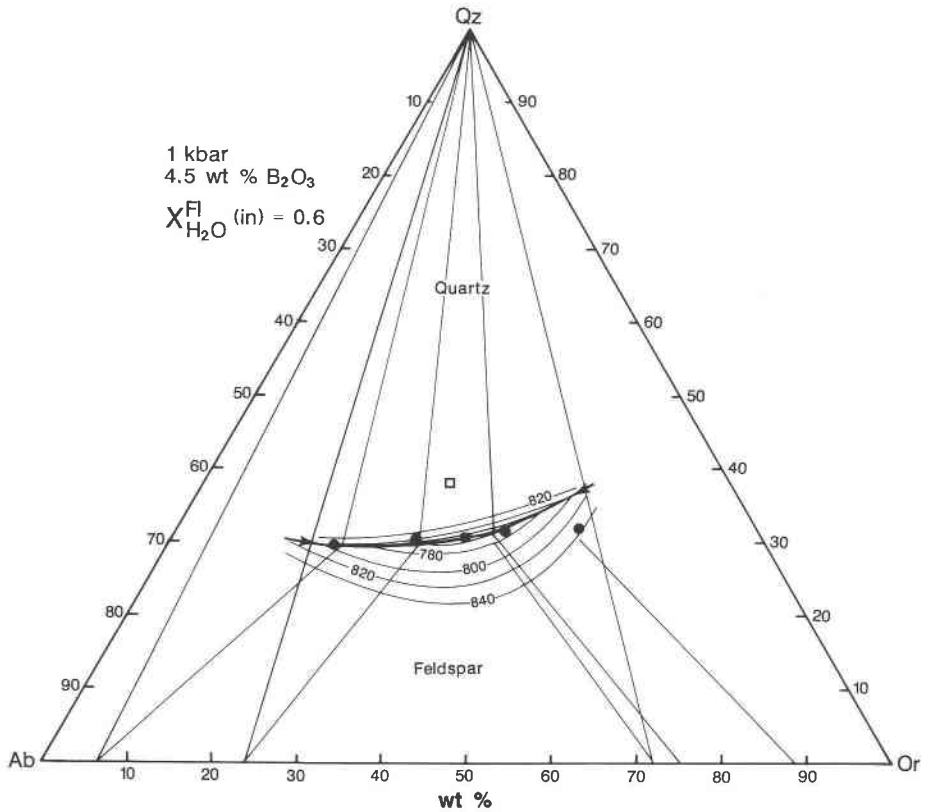

Fig. 4. Liquidus phase relations in the system Qz-Ab-Or at 1 kbar for 4.5 wt% B_2O_3 in the melt under H_2O-undersaturated conditions. Notations, symbols, and sources of data as in Fig. 1.

Al is in fourfold coordination, most of the B has to be in threefold coordination. On the other hand, if Al is removed from the fourfold coordination, an equivalent amount of alkali ions may be used for stabilizing B in fourfold coordination. There are a number of factors governing the coordination of Al in aluminosilicate melts (e.g., McMillan and Piriou, 1983). In the absence of direct spectroscopic information, it is difficult to evaluate the proportion of ^{III}B and ^{IV}B in the borate units for these particular compositions. The analyses of alkali feldspars

TABLE 5.—*Continued*

20	21	21	22	23	24	25	27
760	720	760	740	720	700	720	780
1	2	2	3	4	3	3	1
66.64	64.26	65.96	68.33	67.8	68.28	65.4	64.37
17.63	18.19	17.86	19.21	19.07	18.4	18.51	18.17
12.06	15.0	14.94	0.41	1.13	2.89	12.37	15.0
2.76	1.09	1.42	11.39	10.73	9.49	2.85	0.93
99.09	98.54	100.18	99.34	98.73	99.06	99.13	98.48
6.1	6.0	6.05	6.01	6.01	6.07	6.01	6.01
1.9	2.0	1.93	1.99	1.99	1.93	2.0	2.0
1.41	1.79	1.75	0.05	0.13	0.33	1.45	1.79
0.49	0.2	0.25	1.94	1.84	1.63	0.51	0.17
74	90	88	2	6	17	74	91

indicate that ^{III}B should dominate, as the incorporation of B in feldspar requires the presence of tetrahedrally coordinated B atoms (e.g., Pichavant et al., 1984, and references therein).

The changes in phase relations with the addition of B under H_2O-saturated conditions (lowering of the liquidus temperatures for compositions in the feldspar field, shift of the minimum liquidus compositions toward Ab) suggest that B may cause partial disruption of the aluminosilicate network. Although the precise nature of the structural units involved is not known, this mechanism may be schematically written as

$$B_2O_3 + NaAlSi_3O_8 = BO_3^{3-} + NaBO_2 + Al^{3+} + 3SiO_2. \quad (1)$$

BO_3^{3-} is an isolated unit with B in threefold coordination; $NaBO_2$ a unit with B in fourfold coordination forming part of a larger borate cluster. Al^{3+} represents an Al that has been expelled from tetrahedral coordination and has become a network-modifier. Consequently, an equivalent amount of Na is no longer required for charge balance and may be used for stabilizing a proportion of the B atoms in fourfold coordination, as indicated in the reaction. This reaction, basically analogous to that presented by Burnham and Nekvasil (1986), shows that the main effect of B is to remove alkali cations from the aluminosilicate network. This leads to the partial disruption of

TABLE 6. Composition of glasses coexisting with alkali feldspars and alkali feldspars plus quartz

Glass no.:	6	7	7	8	8	9	10	11	17	18	18	19	19	20	20
Temp (°C):	720	700	710	740	750	780	680	680	700	650	780	650	740	680	740
n:	2	2	2	2	2	3	3	3	2	3	3	3	3	2	5
SiO_2	71.99	71.34	70.89	70.99	71.49	70.35	72.88	72.88	67.93	69.43	71.53	68.40	70.99	67.91	70.69
Al_2O_3	12.29	12.34	12.15	12.14	12.27	12.08	11.61	11.77	12.03	12.12	12.45	11.72	12.58	11.61	12.40
K_2O	3.10	4.39	4.43	5.97	6.15	7.71	3.81	4.38	2.28	2.82	3.25	4.37	4.61	5.51	5.95
Na_2O	5.32	4.5	4.41	3.43	3.43	2.36	4.41	3.81	5.93	5.17	5.5	4.16	4.44	3.25	3.48
Total	92.70	92.57	91.88	92.53	93.34	92.5	92.71	92.84	88.17	89.54	92.73	88.65	92.62	88.28	92.52
Qz	31.5	30.6	30.8	30.5	30.1	29.8	35.2	36.6	28.7	31.9	29.6	31.0	29.7	31.6	29.9
Or	19.8	28.0	28.5	38.1	38.8	48.7	24.3	27.9	15.0	18.6	20.5	29.1	29.4	36.9	38.0
Ab	48.6	41.1	40.6	31.4	31.0	21.3	40.4	34.7	56.0	48.9	49.7	39.7	40.6	31.2	31.8
Co	0.2	0.2	0.1	0.0	0.0	0.0	0.3	0.8	0.0	0.6	0.0	0.2	0.3	0.3	0.3
KS	0.0	0.0	0.0	0.0	0.0	0.1	0.0	0.0	0.1	0.0	0.1	0.0	0.0	0.0	0.0
NaS	0.0	0.0	0.0	0.0	0.0	0.1	0.0	0.0	0.2	0.0	0.1	0.0	0.0	0.0	0.0

Note: Qz = quartz, Or = orthoclase, Ab = albite, Co = corundum, KS = K_2SiO_3, NaS = Na_2SiO_3, *n* = number of microprobe analyses; uncertainties are 0.5% (SiO_2 and Al_2O_3), 2% (K_2O), 3% (Na_2O).

the network, as a fraction of Al can no longer persist in tetrahedral coordination. Reaction 1 consumes $NaAlSi_3O_8$, lowering the activity of the Ab-forming components in the melt. There should exist an equivalent reaction involving $KAlSi_3O_8$, but less in favor of the right-hand term than Reaction 1. This is because the change in phase relations indicates that the Ab-forming components of the melt are preferentially consumed. In addition, experimental results on the composition of aqueous phases in equilibrium with melts (Pichavant, 1981) or alkali feldspars (Pichavant, 1983b) demonstrate that sodium borate complexes are largely dominant over potassium borate complexes in aqueous solutions and thus presumably in melts.

Reaction 1 produces SiO_2 with a corresponding increase in the activity of silica. This may account for the peculiar effect on quartz liquidus temperatures noted in this study (unchanged with addition of B_2O_3), which contrasts with the important reductions usually observed in feldspar-free systems (e.g., a reduction of the quartz liquidus temperature of 215 °C with 4.5 wt% B_2O_3 added in the system SiO_2-B_2O_3; Rockett and Foster, 1965).

The borate groups as in Reaction 1 may be isolated or grouped in larger units, as found in the crystalline alkali borates (e.g., Konijnendijk, 1975b; Pichavant, 1983a). They may also be hydrolyzed, with breaking of the B–O bonds (e.g., Franz, 1966) according to a reaction of the type

$$B_2O_5^{4-} + H_2O = 2HBO_3^{2-}. \quad (2)$$

Reaction 2, written here for a borate group with two ^{III}B, may also apply to borate groups with ^{IV}B. In any case, it leads to a depolymerization of the borate clusters. Reaction 2 accounts for the observed increase of the solubility of H_2O in the melt because the isobaric solubility of water in borate melts is higher than in silicate melts (Franz and Scholze, 1963; Franz, 1966).

Implications for the role of H_2O in aluminosilicate melts

As noted earlier, the "B effect" differs from the "H_2O effect" at 1 kbar. It is worth emphasizing that the latter has been determined by *isobarically* increasing the H_2O content at constant B concentrations. Comparison of the "B effect" with the effect of increasing P_{H_2O} (Tuttle and Bowen, 1958; Luth et al., 1964; Luth, 1976; and Fig. 5) can lead to erroneous conclusions (e.g., Manning et al., 1980; Mysen and Virgo, 1985). This is because increasing P_{H_2O} simultaneously increases pressure (from 0.49 to 10 kbar) and the H_2O content of the melt (from 3 to 17 wt%). Therefore, the phase relations obtained (Fig. 5) reflect the combined effect of both variables rather than the effect of H_2O alone. The individual effect of H_2O at 1 kbar can be deduced from Figure 5. The individual effect of pressure is not well established. From the phase relations available in the dry binary systems Qz-Ab and Qz-Or (Luth, 1969; Boettcher et al., 1984), one can infer a shift of the ternary minimum toward Ab with increasing pressure, in agreement with calculations (Nekvasil and Burnham, 1987).

Although the "H_2O effect" and the "B effect" are different, the change in phase relations in both cases leads

TABLE 7. Compositions and temperatures of minimum liquidus points

	Qz (wt%)	Or (wt%)	Ab (wt%)	*T* (°C)	*P* (kbar)	H_2O (wt%)
H_2O-saturated, B_2O_3-free*	38	29	33	720	0.981	4.4
H_2O-saturated, 1 wt% B_2O_3**	36	27	37	680	1	~4.5
H_2O-saturated, 4.5 wt% B_2O_3**	31	23	46	640	1	~6.5
H_2O-undersaturated, 4.5 wt% B_2O_3**	31	35	34	750	1	2.4–3.2

* From Tuttle and Bowen (1958), Luth (1976).
** Uncertainties: temperature, ±15 °C; compositions, ±1%.

TABLE 6.—*Continued*

20	21	21	22	23	24	25	27
760	720	760	740	720	700	720	780
5	2	5	2	2	2	2	2
71.44	67.91	70.75	68.45	66.74	68.22	66.09	65.05
12.17	11.74	12.00	13.51	13.78	13.85	13.46	13.41
6.02	7.14	7.62	2.00	2.94	4.57	5.82	8.77
3.44	2.27	2.39	6.56	6.35	5.59	4.45	2.16
93.07	89.06	92.76	90.52	89.81	92.23	89.82	89.41
30.5	30.7	30.4	25.0	20.7	20.7	20.5	21.2
38.2	47.4	47.8	13.1	19.3	29.7	37.8	58.0
31.3	21.6	21.5	61.3	59.8	50.2	41.4	20.4
0.0	0.3	0.0	0.6	0.2	0.0	0.0	0.4
0.0	0.0	0.2	0.0	0.0	0.2	0.1	0.0
0.0	0.0	0.1	0.0	0.0	0.2	0.1	0.0

to a reduction of the liquidus volume for Ab relative to Qz and Or. With the addition of F, Manning (1981) also found a similar contraction of the liquidus field for Ab. Therefore, this behavior appears to be a fundamental property of the haplogranite system. It contrasts with that observed in less polymerized systems, which generally show an enlargement of the liquidus volume of less polymerized minerals with increasing H_2O contents (e.g., Kushiro, 1972; Mysen et al., 1980). On the basis of the present experiments, it is suggested that there are similarities among the structural roles of H_2O, F, and B in fully polymerized aluminosilicate melts.

It is generally accepted that H_2O dissolves in fully polymerized melts by hydrolysis with bridging oxygens from the network and production of OH groups (e.g., Burnham, 1979). In addition to these OH groups, molecular H_2O is also present (e.g., Ernsberger, 1977; Stolper, 1982). In the Burnham model (Burnham, 1979), the interaction between H_2O and the network leads to breaking of T–O–T bonds (T = tetrahedrally coordinated cation) and exchange of H^+ for Na^+, with little change in the Al coordination. In contrast, some H_2O-solubility (Oxtoby and Hamilton, 1978) and Raman spectroscopic studies (Mysen et al., 1980) show that dissolution of H_2O is accompanied by expulsion of Al from the tetrahedral coordination. The similarities noted here between the individual effect of B (this study), F (Manning et al., 1980; Manning, 1981) and H_2O (this study) in the Qz-Ab-Or system at 1 kbar further support this hypothesis. In the presence of F, Manning et al. (1980) and Manning (1981) interpreted the observed changes in phase relations to indicate the formation of aluminofluoride complexes. In the presence of B, alkali borate complexes are probably formed (see above). Therefore, F and B form structural units that involve cations previously forming part of the network. In both cases, Al is removed from the aluminosilicate network, either directly (formation of aluminofluoride complexes) or indirectly (formation of alkali borate complexes). This conclusion is supported by some spectroscopic studies (Mysen and Virgo, 1985). The formation of these complexes preferentially consumes the Ab-forming components in the melt, thereby accounting for the observed reductions in the liquidus volume for Ab. By analogy with F and B, the interaction between H_2O and the aluminosilicate network is considered to involve the formation of similar structural units, probably with Na and Si. The existence of such complexes is required by some H_2O-solubility studies (Oxtoby and Hamilton, 1978). Mysen et al. (1980) presented spectroscopic evidence for the existence of complexes between H_2O and alkalis or Si in fully polymerized glasses. In

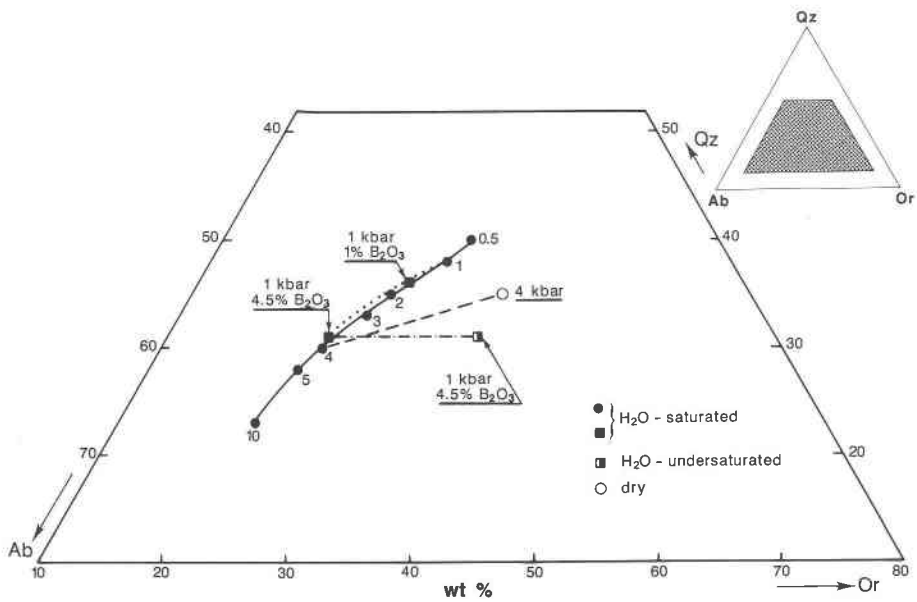

Fig. 5. Projections of the minima and eutectics of the system Qz-Ab-Or for different P_{H_2O} (● labeled with pressure, Luth, 1976), for 1 and 4.5 wt% B_2O_3 in the melt at 1 kbar under H_2O-saturated (■) and undersaturated (◨) conditions (this work). The 4-kbar dry minimum (○) is taken from Steiner et al. (1975).

contrast, Al appears to be unrelated to any hydroxyl group (Oxtoby and Hamilton, 1978; Mysen et al., 1980).

Petrologic applications

The experimental data presented in this paper have important implications for fractionation processes in felsic magmas at low pressures. The petrologic applications may be divided into two groups. The first group is of wide importance for felsic magmatism: it deals with the role of water during differentiation in felsic magmas. The second group of applications more specifically concerns B-rich magmas.

The data and discussion in this paper allow an estimation to be made of the individual effects of pressure and of H_2O content of the melt on the phase relations in the Qz-Ab-Or system. Consequently, the effect of these two independent parameters during fractional crystallization of granitic magmas may be evaluated. A detailed discussion of case studies is unwarranted here. However, there are several possible natural situations where one of these parameters may be changed independently of the other. For example, H_2O enrichment in the melt under roughly isobaric conditions may be a common situation in magma chambers undergoing fractional crystallization of anhydrous phases. In contrast, a magma adiabatically ascending from its source region may undergo a pressure drop without any significant change of the H_2O content. It is worth emphasizing, however, that the "H_2O effect" determined here at 1 kbar may not be necessarily identical at higher pressures. There are also few data concerning the effect of pressure. More work is needed, involving both experiments and calculations, in order to distinguish between the individual effects of pressure and H_2O content of the melt during differentiation of granitic magmas.

With respect to B-bearing magmas, applications concerning their low melting temperatures have been presented elsewhere (Pichavant, 1981) and are clearly strengthened by the liquidus data. Here, the focus is on the effect of B on the composition of residual magmas and on some implications of melt structure.

B is present in elevated concentration in tourmaline leucogranites, aplites, and pegmatites (e.g., Pichavant and Manning, 1984). In these rocks, the average B content (mainly tied up in tourmaline) is around 0.2–0.3 wt% B_2O_3 (Pichavant and Manning, 1984). B may also be found in elevated amounts in some race-element, Li- and F-enriched pegmatites (e.g., Joliff et al., 1986; London, 1986). The amount of tourmaline present in the rock may not be a valid indication of the amount of B in the melt. Tourmaline crystallization is controlled by many other factors than the B content of the melt, including P, T, f_{O_2} and several compositional factors (Benard et al., 1985). B may also be lost to the vapor phase because of its melt/vapor partition coefficient (see above). More direct information regarding the B content of natural felsic melts may be obtained from the composition of some obsidian glasses. The Macusani glasses from southeastern Peru are peraluminous obsidians of granitic composition; they contain up to 0.62 wt% B_2O_3 (Pichavant et al., 1987, and references therein) and may be useful to establish a possible upper limit of B_2O_3 concentrations in natural felsic magmas at around 1 wt%.

The CIPW normative composition of some selected B-rich felsic rocks is plotted in Figure 6, together with minimum liquidus compositions in the H_2O-saturated Qz-Ab-Or system, with and without added B. The rocks plotted are characterized by magmatic tourmaline crystallization. Therefore, the B enrichment is related to magmatic processes, as opposed to hydrothermal tourmalinization (e.g., Charoy, 1982). The normative compositions generally cluster near the B-free, low P_{H_2O} minima of the Qz-Ab-Or system (see also Pichavant and Manning, 1984). This is consistent with crystallization at low pressures, under roughly H_2O-saturated conditions for most of the rocks plotted (one Manaslu leucogranite plots close to the 3-kbar P_{H_2O} minimum). There is no systematic shift of the normative compositions toward Ab, in contrast to that observed for the F-rich magmatic rocks (Kovalenko and Kovalenko, 1976; Manning, 1982; Christiansen et al., 1984; Pichavant and Manning, 1984). This is consistent with the phase relations determined in this paper: the minimum liquidus composition with 1 wt% B_2O_3 added is not drastically shifted from the 1-kbar P_{H_2O} minimum (Fig. 1). It is therefore concluded that the B concentration of natural magmas is too low to have any large effect on the major-element composition of residual melts.

However, B enrichment in natural magmas may be accompanied by enrichment in F and Li, as in some rare-element pegmatites (e.g., London, 1987). The Macusani glasses (compositionally equivalent to some rare-element pegmatite magmas, London, 1987; Pichavant et al., 1987) are remarkable examples of this behavior: besides 0.62 wt% B_2O_3, they contain up to 1.3 wt% F and 0.74 wt% Li_2O (London, 1987; Pichavant et al., 1987). The normative composition of a Macusani glass (Fig. 6) reflects the combined effects of B, F, and Li on phase relations and composition of residual liquids (Pichavant et al., 1987). Therefore, the effects of components such as F and Li may combine with the effect of B to affect significantly crystal $\rightleftharpoons$ liquid equilibria and the composition of residual felsic liquids.

As detailed above, B causes a major reorganization of melt structure: the aluminosilicate network is partially disrupted with the formation of structural units that involve cations derived from the network; network-modifying cations are created in this process. The overall effect is to promote depolymerization of the melt with important consequences for its physical and chemical properties. Liquidus (and solidus) temperatures are reduced. Viscosities are expected to be decreased and diffusion coefficients to be increased. Crystal/liquid partition coefficients may also decrease, and the solubilities of high field-strength cations (e.g., Sn, W, Ta, U) may increase because depolymerization creates structurally favorable sites in the melt. The solubility of some "refractory phas-

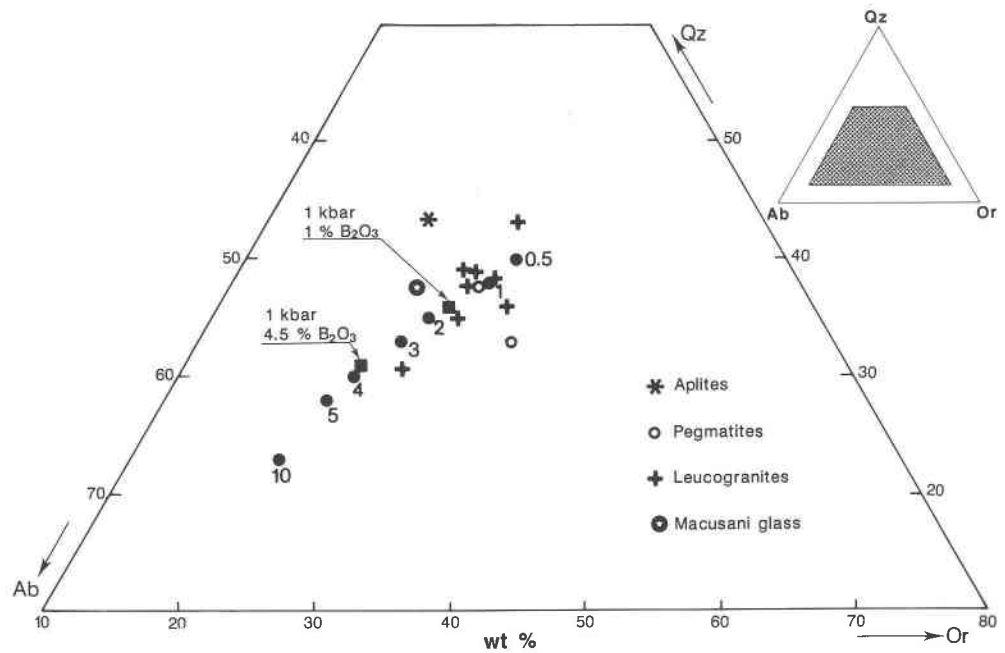

Fig. 6. CIPW normative composition of selected B-rich granitic rocks, compared with H_2O-saturated minima and eutectics in the Qz-Ab-Or system (symbols as in Fig. 5). Sources of data: Tourmaline leucogranites—Dietrich and Gansser (1981), Le Fort (1981), Pichavant and Manning (1984), Benard et al. (1985), Gouanvic and Gagny (1985). Tourmaline pegmatites—Manning (unpub.), Pichavant and Manning (1984). Tourmaline aplite—Nemec (1978). Macusani glass—Pichavant et al. (1987).

es" may also increase as a result of the formation of additional structural units. Therefore, the minor- and trace-element chemistry of the liquid may be profoundly modified, in contrast with modest changes for the major elements. A better knowledge of the structure of residual felsic magmas is clearly necessary before attempting to model their chemical and physical properties.

Acknowledgments

David Manning is gratefully acknowledged for the experimental runs, for many discussions, and for review of the final manuscript. Many stimulating discussions and a very careful review of the final manuscript by C. Wayne Burnham led to improvement of this paper. However, the interpretations and conclusions are the author's responsibility. Discussions and reviews of early drafts by Bernard Charoy and Mike Henderson were helpful. Final presentation was improved by the comments of M. Barton, D. Burt, and F. Spera. David London is acknowledged for sending preprints and reprints. Hanna Nekvasil provided the calculations of H_2O contents. This study was supported by CNRS, A.T.P. Géochimie et Métallogénie 1981. CRPG Contribution No. 714.

References cited

Benard, F., Moutou, P., and Pichavant, M. (1985) Phase relations of tourmaline leucogranites and the significance of tourmaline in silicic magmas. Journal of Geology, 93, 271–291.

Boettcher, A.L. (1984) The system SiO_2-H_2O-CO_2: Melting, solubility mechanisms of carbon, and liquid structure to high pressures. American Mineralogist, 69, 823–833.

Boettcher, A., Guo, Q., Bohlen, S., and Hanson, B. (1984) Melting in feldspar-bearing systems to high pressures and the structures of aluminosilicate liquids. Geology, 12, 202–204.

Burnham, C.W. (1979) The importance of volatile constituents. In H.S. Yoder, Jr., Ed., The evolution of the igneous rocks, p. 439–482. Princeton University Press, Princeton, New Jersey.

Burnham, C.W., and Nekvasil, H. (1986) Equilibrium properties of granite pegmatite magmas. American Mineralogist, 71, 239–263.

Charoy, B. (1982) Tourmalinization in Cornwall, England. In A.M. Evans, Ed., Metallization associated with acid magmatism, p. 63–70. Wiley, New York.

Chorlton, L.B., and Martin, R.F. (1978) The effect of boron on the granite solidus. Canadian Mineralogist, 16, 239–244.

Christiansen, E.H., Bikun, J.V., Sheridan, M.F., and Burt, D.M. (1984) Geochemical evolution of topaz rhyolites from the Thomas Range and Spor Mountain, Utah. American Mineralogist, 69, 223–236.

Dietrich, V., and Gansser, A. (1981) The leucogranites of the Bhutan Himalaya. Schweizerische Mineralogische und Petrographische Mitteilungen, 61, 177–202.

Ernsberger, F.M. (1977) Molecular water in glass. American Ceramic Society Journal, 60, 91–92.

Fenn, P.M. (1977) The nucleation and growth of alkali feldspars from hydrous melts. Canadian Mineralogist, 15, 135–161.

Franz, H. (1966) Solubility of water vapour in alkali borate melts. American Ceramic Society Journal, 49, 473–477.

Franz, H., and Scholze, H. (1963) Die Löslichkeit von H_2O—Dampf in glass schmelzen verschiedener Basizität. Glastechnische Berichte, 36, 347–355.

Gouanvic, Y., and Gagny, C. (1985) Reflexion sur l'utilisation des expérimentations pour la compréhension de la genèse des aplopegmatites litées (cas de Santa Comba)—Réponse à la discussion de M. Pichavant (1984). Bulletin de la Société Géologique de France, 8, 273–276.

Huang, W.L., and Wyllie, P.J. (1975) Melting reactions in the system $NaAlSi_3O_8$-$KAlSi_3O_8$-SiO_2 to 35 kilobars, dry and with excess water. Journal of Geology, 83, 737–748.

Johannes, W. (1980) Metastable melting in the granite system Qz-Or-Ab-An-H_2O. Contributions to Mineralogy and Petrology, 72, 73–80.

——— (1985) The significance of experimental studies for the formation of migmatites. In J.R. Ashworth, Ed., Migmatites, p. 36–85. Blackie, Glasgow, Scotland.

Jolliff, B.L., Papike, J.J., and Shearer, C.K. (1986) Tourmaline as a recorder of pegmatite evolution: Bob Ingersoll pegmatite, Black Hills, South Dakota. American Mineralogist, 71, 472–500.

Konijnendijk, W.L. (1975a) Structural differences between borosilicate and aluminosilicate glasses studied by Raman scattering. Glastechnische Berichte, 48, 216–218.

——— (1975b) The structure of borosilicate glasses. Philips Research Reports Supplement 1, Eindhoven.

Kovalenko, V.I., and Kovalenko, N.I. (1976) Ongonites (topaz-bearing quartz keratophyres): Subvolcanic analogues of rare-metal Li-F granites. Joint Soviet-Mongolian Scientific Research Geological Expedition, Nauka, Moscow.

Kushiro, I. (1972) Effect of water on the composition of magmas formed at high pressures. Journal of Petrology, 13, 311–334.

Lagache, M., and Weisbrod, A. (1977) The system two alkali feldspars–KCl–NaCl–H_2O at moderate to high temperatures and low pressures. Contributions to Mineralogy and Petrology, 62, 77–102.

Le Fort, P. (1981) Manaslu leucogranite: A collision signature of the Himalaya. A model for its genesis and emplacement. Journal of Geophysical Research, 86, 10545–10568.

London, D. (1986) Magmatic-hydrothermal transition in the Tanco rare-element pegmatite: Evidence from fluid inclusions and phase-equilibrium experiments. American Mineralogist, 71, 376–395.

——— (1987) Internal evolution of rare-element pegmatites: Effects of F, B, Li and P. Geochimica et Cosmochimica Acta, 51, 403–420.

Luth, W.C. (1969) The system $NaAlSi_3O_8$-SiO_2 and $KAlSi_3O_8$-SiO_2 to 20 kb and the relationships between H_2O content, P_{H_2O} and P_{total} in granitic magmas. American Journal of Science, 267-A, 325–341.

——— (1976) Granitic rocks. In D.K. Bailey and R. MacDonald, Eds., The evolution of the crystalline rocks, p. 335–417. Academic Press, London.

Luth, W.C., Jahns, R.H., and Tuttle, O.F. (1964) The granite system at pressures of 4 to 10 kilobars. Journal of Geophysical Research, 69, 759–773.

Manning, D.A.C. (1981) The effect of fluorine on liquidus phase relationships in the system Qz-Ab-Or with excess water at 1 kbar. Contributions to Mineralogy and Petrology, 76, 206–215.

——— (1982) An experimental study of the effects of fluorine on the crystallization of granitic melts. In A.M. Evans, Ed., Metallization associated with acid magmatism, p. 191–203. Wiley, New York.

Manning, D.A.C., Hamilton, D.L., Henderson, C.M.B., and Dempsey, M.J. (1980) The probable occurrence of interstitial Al in hydrous, F-bearing and F-free aluminosilicate melts. Contributions to Mineralogy and Petrology, 75, 257–262.

McMillan, P., and Piriou, B. (1983) Raman spectroscopic studies of silicate and related glass structure: A review. Bulletin de Minéralogie, 106, 57–75.

Montel, J.-M. (1986) Experimental determination of the solubility of Ce-monazite in SiO_2-Al_2O_3-K_2O-Na_2O melts at 800 °C, 2 kbar, under H_2O-saturated conditions. Geology, 14, 659–662.

Mysen, B.O., and Virgo, D. (1985) Structure and properties of fluorine-bearing aluminosilicate melts: The system Na_2O-Al_2O_3-SiO_2-F at 1 atm. Contributions to Mineralogy and Petrology, 91, 205–220.

Mysen, B.O., Virgo, D., Harrison, W.J., and Scarfe, C.M. (1980) Solubility mechanisms of H_2O in silicate melts at high pressures and temperatures: A Raman spectroscopic study. American Mineralogist, 65, 900–914.

Nekvasil, H., and Burnham, C.W. (1987) The calculated individual effects of pressure and water content on phase equilibria in the granite system. In B.O. Mysen, Ed., Magmatic processes: Physiochemical principles, Geochemical Society Special Publication 1, 433–445.

Nemec, D. (1978) Genesis of aplite in the Ricany massif, central Bohemia. Neues Jahrbuch für Mineralogie Abhandlungen, 132, 322–339.

Oestrike, R., Geisinger, K., Navrotsky, A., Turner, G.L., and Kirkpatrick, R.J. (1986) Structure and thermochemistry of glasses along the join $NaAlSi_3O_8$-$NaBSi_3O_8$: The effect of boron. Geological Society of America Abstracts with Programs, 18, 709.

Oxtoby, S., and Hamilton, D.L. (1978) The discrete association of water with Na_2O and SiO_2 in NaAl silicate melts. Contributions to Mineralogy and Petrology, 66, 185–188.

Pichavant, M. (1981) An experimental study of the effect of boron on a water-saturated haplogranite at 1 kbar pressure: Geological applications. Contributions to Mineralogy and Petrology, 76, 430–439.

——— (1983a) Melt-fluid interaction deduced from studies of silicate-B_2O_3-H_2O systems at 1 kbar. Bulletin de Minéralogie, 106, 201–211.

——— (1983b) (Na,K) exchange between alkali feldspars and aqueous solutions containing borate and fluoride anions; experimental results at $P = 1$ kbar (abs.). 3rd NATO Advanced Study Institute on Feldspars, Feldspathoids and their Parageneses.

Pichavant, M., and Manning, D.A.C. (1984) Petrogenesis of tourmaline granites and topaz granites: the contribution of experimental data. Physics of the Earth and Planetary Interiors, 35, 31–50.

Pichavant, M., and Ramboz, C. (1985a) Liquidus phase relationships in the system Qz-Ab-Or-B_2O_3-H_2O at 1 kbar under H_2O-undersaturated conditions and the effect of H_2O on phase relations in the haplogranite system (abs.). Terra Cognita, 5, 230.

——— (1985b) Première détermination expérimentale des relations de phases dans le système haplogranitique en conditions de sous-saturation en H_2O. Comptes Rendus de l'Académie des Sciences, 301, 607–610.

Pichavant, M., Schnapper, D., and Brown, W.L. (1984) Al⇌B substitution in alkali feldspars; preliminary hydrothermal data in the system $NaAlSi_3O_8$-$NaBSi_3O_8$. Bulletin de Minéralogie, 107, 529–537.

Pichavant, M., Valencia Herrera, J., Boulmier, S., Briqueu, L., Joron, J.L., Juteau, M., Marin, L., Michard, A., Sheppard, S.M.F., Treuil, M., and Vernet, M. (1987) The Macusani glasses, SE Peru: Evidence of chemical fractionation in peraluminous magmas. In B.O. Mysen, Ed., Magmatic processes: Physicochemical principles, Geochemical Society Special Publication 1, 359–373.

Rockett, T.J., and Foster, W.R. (1965) Phase relations in the system SiO_2-B_2O_3. American Ceramic Society Journal, 48, 75–80.

Shaw, H.R. (1974) Diffusion of H_2O in granitic liquid. I—Experimental data. II—Mass transfer in magma chambers. In A.W. Hofmann, B.J. Giletti, H.S. Yoder, Jr., and R.A. Yund, Eds., Geochemical transport and kinetics. Carnegie Institution of Washington Publication 634, p. 139–170.

Smith, P., and Parsons, I. (1974) The alkali feldspar solvus at 1 kbar water vapour pressure. Mineralogical Magazine, 39, 747–767.

Steiner, J.C., Jahns, R.H., and Luth, W.C. (1975) Crystallization of alkali feldspar and quartz in the haplogranite system $NaAlSi_3O_8$-$KAlSi_3O_8$-SiO_2-H_2O at 4 kb. Geological Society of America Bulletin, 86, 83–98.

Stolper, E. (1982) Water in silicate glasses: An infrared spectroscopic study. Contributions to Mineralogy and Petrology, 81, 1–17.

Swanson, S.E. (1977) Relation of nucleation and crystal-growth rate to the development of granitic textures. American Mineralogist, 62, 966–978.

Swanson, S.E., and Fenn, P.M. (1986) Quartz crystallization in igneous rocks. American Mineralogist, 71, 331–342.

Thompson, J.B., Jr., and Waldbaum, D.R. (1968) Mixing properties of sanidine crystalline solutions. I—Calculations based on ion exchange data. American Mineralogist, 53, 1965–1999.

Tuttle, O.F., and Bowen, N.L. (1958) Origin of granite in the light of experimental studies in the system $NaAlSi_3O_8$-$KAlSi_3O_8$-SiO_2-H_2O. Geological Society of America Memoir 74.

Whitney, J.A. (1975) The effects of pressure, temperature and $X(H_2O)$ on phase assemblage in four synthetic rock compositions. Journal of Geology, 83, 1–31.

Wyllie, P.J., and Tuttle, O.F. (1960) Experimental investigation of silicate systems containing two volatile components: I—Geometrical considerations. American Journal of Science, 258, 497–517.

——— (1961) Experimental investigation of silicate systems containing two volatile components: II—The effects of NH_3 and HF, in addition to H_2O, on the melting temperatures of albite and granite. American Journal of Science, 259, 128–143.

Manuscript received March 19, 1987
Manuscript accepted June 26, 1987